

# Entropic Interactions in Soft Nanomaterials

T. Bickel<sup>1,\*</sup> and C. M. Marques<sup>2</sup>

<sup>1</sup>CPMOH, UMR 5798 CNRS – Université Bordeaux I, 351 cours de la Libération, 33400 Talence, France

<sup>2</sup>Institut Charles Sadron, UPR 022 CNRS-ULP, 6 rue Boussingault, 67083 Strasbourg Cedex, France

We review the forces that rule interactions between phospholipid membranes and other soft nanomaterials such as polymers and colloids. Contrary to traditional nanostructures, soft materials display a high susceptibility to the fluctuations of the thermal environment, leading to new forces of an essentially entropic nature.

**Keywords:** Soft Materials, Nanoparticles, Stealth Liposomes.

## 1. INTRODUCTION

Phospholipids self-assemble in solution as fluid bilayers of typically 5 nm thickness, leading to lamellae structures of planar, cylindrical, spherical, or even more complex geometries.<sup>1–3</sup> When the bilayers enclose an inner spherical or cylindrical space one refers to these assemblies as vesicles or liposomes.<sup>4</sup> In the living realm, where phospholipid bilayers build the walls of cells and cellular organelles,<sup>5</sup> vesicles and liposomes provide simple models to understand cell wall properties: Transport, fusion, mechanical resistance . . . Depending on the actual self-assembly conditions, single or multiple layer vesicles can be prepared in a large size range, from liposomes as small as a few tens of nanometers to giant vesicles as large as one tenth of a millimeter. The physics of simple fluid bilayers is now well understood. Following seminal work by Helfrich,<sup>6</sup> who first recognized the importance of the membrane bending elasticity, extensive theoretical and experimental studies contributed to the writing of one of the finest chapters in modern statistical physics of soft condensed matter.<sup>7</sup> Interestingly, fluid bilayers also inspired many fundamental studies in Mathematics, particularly in topology and differential geometry, some of these studies bearing a direct impact on the physical description of the membranes.

Fluid membranes often contain also other macromolecular species. Biological bilayers host proteins responsible for functions as diverse as anchoring the cytoskeleton, providing coating protection against the body immune response or opening ionic channels for osmotic compensation.<sup>8</sup> In cosmetics, pharmaceuticals, or detergency, many formulations are membrane solutions with polymers added for performance, processing, conditioning, or delivery.<sup>9–16</sup> An interesting example of a polymer membrane system has been recently developed in the field of drug delivery.

Indeed, the capacity of the liposomes to encapsulate a great variety of active molecules has prompted many studies to test the possibility of actually delivering drugs through liposome carriers, but it was not until a solution was found to avoid recognition and elimination by the immune system that the first anti-cancer drugs were approved and marketed. This solution involves polymer membrane interactions and is an interesting example of cross-fertilization between applied studies in pharmacology and more fundamental research in the field of colloidal forces. In fact, in many industrial applications such as paints, lubrication oils, and food suspensions one might want to prevent aggregation of the suspended particles. This is many times achieved by coating the colloid surface with a polymer layer, that prevents bead–bead contact. It was also found that these coatings, shown in Figure 1, prevented immediate recognition of liposomes by the immune system, therefore increasing the liposome circulation times and making possible drug transport in the blood.

The problems risen by the development of stealth liposome technology<sup>17</sup> are a good illustration of the fundamental questions addressed in this review. Indeed, locating, identifying, and controlling the forces that act between a membrane and other soft nano-materials such as colloids and polymers are crucial steps not only in the field of drug delivery, but also for a much larger class of natural and industrial systems. In the following, we describe recent progresses in the theoretical understanding of the interactions between phospholipid membranes and other soft objects of the nanometer world.

## 2. ELASTIC PROPERTIES OF FLUID MEMBRANES

Systems built from fluid membranes exhibit a wide variety of shapes and topologies that can be well understood within the framework of curvature elasticity.<sup>18</sup> The surface

\*Author to whom correspondence should be addressed.

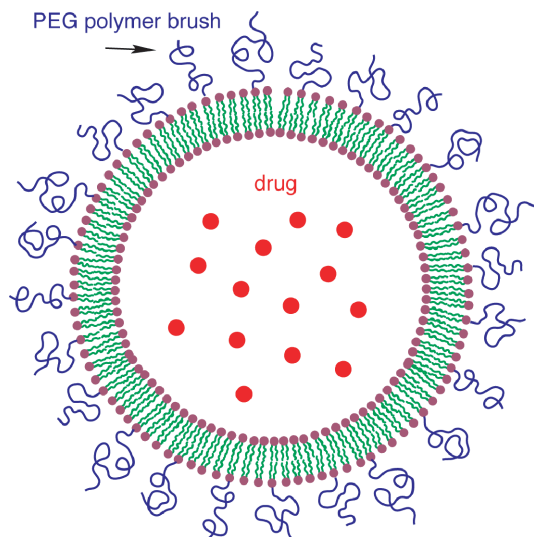


**Fig. 1.** The stealth liposome concept. A polymer protective layer avoids recognition by the immune system and allows a prolonged circulation in the blood.

energy density associated with curvature effects can be written as<sup>6</sup>

$$h(R_1, R_2) = \frac{\kappa}{2} \left( \frac{1}{R_1} + \frac{1}{R_2} - \frac{2}{R_0} \right)^2 + \frac{\bar{\kappa}}{R_1 R_2} \quad (1)$$

where  $R_1$  and  $R_2$  are the local radii of curvature that describe the shape of the membrane, and  $R_0$  is the local radius of spontaneous curvature, an intrinsic property of each membrane system. For instance, the spontaneous curvature  $R_0^{-1}$  vanishes for symmetric membranes.  $\kappa$  and  $\bar{\kappa}$  are the membrane elastic constants that have dimensions of energy. The curvature rigidity  $\kappa$  controls the amplitude of thermal fluctuations. Experimental  $\kappa$  values for fluid bilayers are found in the range of one to several tens of  $k_B T$  units. The Gaussian curvature rigidity  $\bar{\kappa}$  plays an important role in the determination of the membrane topology. Indeed, according to the Gauss-Bonnet theorem, the total energy contribution from the Gaussian curvature is a topological constant:

$$\int dS (R_1 R_2)^{-1} = 4\pi(1 - g)$$

where  $g$  is the surface topological genus ( $g = 0$  for a sphere,  $g = 1$  for a torus).  $\bar{\kappa}$  can thus be described as a chemical potential conjugated to surface topology.

The practical usefulness of membranes relies on the possibility of controlling the shape and topology of the formulated structures. A given geometry, or a set of different geometries interchangeable by phase transformations, is not only fixed by the values of the elastic constants but is also the result of the interplay between several different parameters such as the temperature, the osmotic pressure, the ionic strength... However, in many situations these parameters can not be freely modified, and it is then better to directly tune the elastic constants themselves. Many recent theoretical and experimental studies have thus been

devoted to the contribution of colloid and polymer solutions to the surface energy of fluid bilayers. We will now present an overview of the main results of these studies. In this section we first recall a general method widely used for the determination of the effective elastic constants, and describe in the following sections several different experimental situations: Depletion of flexible and rigid objects, polymer adsorption... We will conclude by an extensive review of polymer decorated membranes, describing first the average modifications of the elastic curvature constants and then the local forces that the polymer apply to the membrane.

## 2.1. Effective Elastic Constants

For a bare membrane, in the absence of colloids, the Helfrich energy can be easily computed for simple geometries. The energy per unit surface of a sphere of radius  $R_1 = R_2 = R$  is

$$\Delta h_s(R) = -\frac{4\kappa c_0}{R} + \frac{2\kappa + \bar{\kappa}}{R^2} \quad (2)$$

where  $\Delta h_s(R) = h_s(R) - h_s(\infty)$ . For a cylinder,  $R_1 = R$  and  $R_2 = \infty$ , one has

$$\Delta h_c(R) = -\frac{2\kappa c_0}{R} + \frac{\kappa}{2R^2} \quad (3)$$

It is worth noting that there is a factor two between the linear terms of the cylinder and sphere surface energies, a general geometric feature that holds for all surface energy densities with analytical expansions in  $1/R$ .

In the vicinity of an interface, wall particle interactions lead to a perturbation of the structure of the colloidal suspension over a distance comparable to the particle size. In the neighborhood of an interface, the properties of a colloidal solution are modified over a typical distance of the order of  $r_0$ , the size of the colloidal particles. This perturbation increases the system energy proportionally to the area of the interface. When the surface is slightly curved, such excess surface energy can be expanded in powers of  $r_0 R^{-1} \ll 1$ . The renormalization of the elastic curvature constants can then be obtained by comparing the first two terms of the expansion to the Helfrich energy. In the following, we consider only bare symmetric membranes for which the spontaneous curvature vanishes,  $c_0 = 0$ ; results for cases where  $c_0 \neq 0$  can be obtained in a similar manner. Formally, the excess energy expansion for a sphere ( $i = s$ ) or a cylinder ( $i = c$ ) is

$$\gamma_i(R) = \lambda_i + \frac{\mu_i}{R} + \frac{\nu_i}{R^2} \quad (4)$$

The curvature dependent terms of the excess surface energy of a membrane in contact with the colloidal environment can be written as

$$\Delta f_s(R) = \Delta h_s(R) + \Delta \gamma_s(R) = -\frac{4\kappa \Delta c_0}{R} + \frac{2\kappa_{\text{eff}} + \bar{\kappa}_{\text{eff}}}{R^2} \quad (5)$$

$$\Delta f_c(R) = \Delta h_c(R) + \Delta \gamma_c(R) = -\frac{2\kappa \Delta c_0}{R} + \frac{\kappa_{\text{eff}}}{2R^2} \quad (6)$$

for the sphere and the cylinder, respectively. Exposure of one side only of the membrane to the particle surface interaction induces a spontaneous curvature that can be written as

$$\Delta c_0 = \frac{\mu_s}{4\kappa} = \frac{\mu_c}{2\kappa} \quad (7)$$

A positive contribution indicates a tendency of the membrane to spontaneously bend towards the solution, the sphere having a negative curvature within our sign convention. When the membrane is embedded in the solution, with both sides exposed to the same colloidal solution, the spontaneous curvature vanishes, since the excess surface energy is the sum of the two contributions  $\Delta\gamma_i = \Delta\gamma_i(R) + \Delta\gamma_i(-R)$ . This leads to

$$\Delta\kappa = \kappa_{\text{eff}} - \kappa = 4\nu_c \quad (8)$$

$$\Delta\bar{\kappa} = \bar{\kappa}_{\text{eff}} - \bar{\kappa} = 2\nu_s - 8\nu_c \quad (9)$$

We will now review different results obtained with this general method by several authors. We will also provide a short theoretical background for each of the experimental situations considered, a more detailed description can of course be found in the relevant literature.<sup>24–26</sup>

### 3. NANOPARTICLE DEPLETION

#### 3.1. Depletion of Rigid Particles: Rods and Spheres

The extraction of tobacco mosaic virus (TMV) and the subsequent observation of the nematic phase in low concentration TMV solutions,<sup>27</sup> triggered a deep interest for suspensions of rigid macromolecules. The isotropic nematic transition in rod solutions was first predicted by Onsager to occur at the rather small concentration  $\rho_b^* = 4.2L^{-2}D^{-1}$ , with  $L$  the rod length and  $D$  its diameter.<sup>28</sup> The depletion interaction of infinitely thin rods and curved walls was first considered by Auvray,<sup>29</sup> then by Yaman et al.<sup>30</sup> These last authors have in particular determined the contribution of the depletion interactions to the elastic constants of the membranes.

One can easily show that the rod depletion layers can significantly modify the membrane elasticity, by comparing the effects of rod and sphere depletion. In a solution of hard spheres of radius  $r_0$  and number density  $\rho_b$ , the typical scale for the energy density is  $k_B T \rho_b$ . The order of magnitude of the excess surface energy is thus  $\Delta\gamma \simeq k_B T \rho_b r_0$ . Typical values for the interfacial tensions are of order  $\gamma_0 \simeq k_B T/a^2$ , where  $a$  is a microscopic size. For a characteristic value  $a = 0.1$  nm,  $\gamma_0$  is of order of a few mN/m. The corrections due to the depletion of spherical particles are thus a factor  $(a/r_0)^2$  lower than typical interfacial tensions even at volume fractions  $\phi = \rho_b(4\pi/3)r_0^3$  of order unity. Corrections to the curvature modulus are of order  $\Delta\kappa \simeq k_B T \rho_b r_0^3$ : Even for the largest possible volume fractions this contribution is only of order  $k_B T$ , a value at the lower end of the range,  $1\text{--}20k_B T$ , for most bare elastic constants. In the case of a rod solution with

rod number density  $\rho_b$ , the upper concentration limit of the isotropic solution is the Onsager concentration  $\rho_b^*$ . The contributions to the interfacial tension are now of the order  $\Delta\gamma \simeq k_B T \rho_b L$ , but even for rod diameters of order of the microscopic length  $a$  the contribution to the interfacial tension of rod solutions at the Onsager concentration is still a factor  $(a/L)$  smaller than typical interfacial tension values. However, modifications of the elastic constants are here of order  $\Delta\kappa \simeq k_B T \rho_b L^3$ , a factor  $(L/D)$  larger than  $k_B T$ . Therefore, even rather rigid phospholipid membranes with elastic constants as large as  $20k_B T$  may have their rigidities substantially modified at low rod concentrations where rod–rod interactions are still negligible.

Technically, Yaman et al. considered an ideal gas of rods of length  $L$  in the presence of flat and curved surfaces which repel the rods.<sup>30,31</sup> They parameterize the possible rod configurations by the center of mass coordinates  $\vec{r}$ , and by two angles specifying the rod direction,  $\omega \equiv (\theta, \phi)$ . The relevant potential describing the thermodynamics of the system is written as:

$$F[\rho(\mathbf{r}, \omega)] = \int d\mathbf{r} d\omega \rho(\mathbf{r}, \omega) (\ln(v\rho/e) - (\mu_b - U_{\text{ext}})) \quad (10)$$

where  $\rho$  is the local concentration,  $v$  a normalization volume,  $\mu_b$  is the solution chemical potential, and  $U_{\text{ext}}$  the interaction potential between the rods and the surface. Functional minimization of  $\Omega$  with respect to  $\rho(\vec{r}, \omega)$  gives the equilibrium density profile. The excess surface energy is given by

$$\begin{aligned} \Delta\gamma &= \frac{1}{\mathcal{F}} (F[\rho(z)] - F[\rho(z \rightarrow \infty)]) \\ &= \int dz [\rho_b - \rho(z)] J(z, R) \end{aligned} \quad (11)$$

where  $S$  is the surface area,  $z$  the perpendicular distance from the surface, and  $J(z, R)$  is the appropriate Jacobian for the geometry. For flat surfaces  $J(z, R) = 1$ , for the outside of a cylinder of radius  $R$ ,  $J(z, R) = 1 + z/R$ , and for the outside of a sphere  $J(z, R) = (1 + z/R)^2$ . Equation (11) holds for both spherical and rodlike particles provided that the corresponding concentration profile is known.

##### 3.1.1. Nanobeads

In the case of hard sphere solutions, where there is no coupling between configuration and curvature. One finds, to second order in curvature, the following correction to the interfacial energy

$$\Delta\gamma_s = k_B T \rho_b r_0 \left( 1 + \frac{r_0}{R} + \frac{r_0^2}{3R^2} \right) \quad (12)$$

$$\Delta\gamma_c = k_B T \rho_b r_0 \left( 1 + \frac{r_0}{2R} \right) \quad (13)$$

The renormalized values of the elastic constants can be directly obtained from Eqs. (8) and (9). If the membrane is exposed on both sides to a bead solution there is no

spontaneous curvature, the elastic constant read:

$$\Delta\kappa = 0 \quad (14)$$

$$\Delta\bar{\kappa} = \frac{2}{3}k_B T \rho_b r_0^3 \quad (15)$$

A different nanobead concentration on both sides of the membrane will lead to a spontaneous curvature, as discussed in the Refs. [32, 33].

### 3.1.2. Rods

The geometrical constraints depend on the convexity of the surface. Yaman et al. gave the following values for the surface energy:

$$\Delta\gamma_{\text{out}} = k_B T \rho_b \frac{L}{4} \quad (16)$$

when the rods interact with a convex surface and

$$\Delta\gamma_{\text{in}} = k_B T \rho_b \frac{L}{4} \left(1 - \alpha \frac{L^2}{R^2}\right) \quad (17)$$

when the rods interact with concave spherical ( $\alpha = 1/2$ ) or cylindrical ( $\alpha = 1/32$ ) surfaces. The asymmetry of the expressions for convex and concave surfaces shows that a membrane will spontaneously bend towards a rod solution, even if there is no spontaneous curvature in the traditional sense. For a membrane immersed in a rod solution one extracts the new elastic constant values

$$\Delta\kappa = -\frac{1}{64}k_B T \rho_b L^3 = -k_B T \frac{\rho_b}{\rho_b^*} \frac{1}{15.2} \frac{L}{D} \quad (18)$$

$$\Delta\bar{\kappa} = \frac{1}{96}k_B T \rho_b L^3 = k_B T \frac{\rho_b}{\rho_b^*} \frac{1}{22.9} \frac{L}{D} \quad (19)$$

$\kappa$  decreases and  $\bar{\kappa}$  increases, with an amplitude  $L/D$  times larger than  $k_B T$  as anticipated: A rod solution might in principle destabilize a fluid membrane by lowering its curvature rigidity.

### 3.2. Depletion of Flexible Polymers

Having described depletion of rigid nanoparticles, we now consider the opposite case of flexible polymers, a paradigmatic example of soft nanoparticles. Statistical methods have been used to describe the physics of macromolecules since the work of Kuhn around 1930: Polymers are then represented as gaussian random walks.<sup>34</sup> In 1949, Flory describes effects of excluded volume in the polymers<sup>35</sup> and realizes that the chains are swollen with respect to the corresponding gaussian state. Flory estimation of the chain swelling is based on a simple balance between chain stretching and excluded volume interactions: The radius of a three dimensional chain is given by  $R^2 \propto N^{2\nu} a^2$  with  $\nu = 3/5$ . New important contributions to the theoretical description of polymer chains arise in the sixties, and emerging numerical methods will later allow to test the theoretical descriptions of self-avoiding random walks. Edwards introduces in 1965 a self-consistent

theoretical field description of the polymer chains providing a systematic method to account for intra and inter-chain interactions.<sup>36</sup> The modern description of polymer chains is introduced by de Gennes in 1972.<sup>37</sup> de Gennes shows that the partition function of a polymer chain is connected by a simple mathematical transformation to the partition function as a particular spin system. This strong connection to critical phenomena has allowed to understand polymer chain behavior at the light of renormalization group theory. In particular, it can be shown that the upper critical space dimension for polymers is  $d = 4$ . Above this upper critical dimension the excluded volume correlations become irrelevant and chain behavior is well described by gaussian statistics. Chain properties can therefore be extracted by renormalization group methods based on the so called  $\epsilon$ -expansion close to the upper critical dimension. For instance, a perturbation expansion in  $\epsilon = 4 - d$  to second order gives  $\nu = 1/2(1 + 1/8\epsilon + 15/256\epsilon^2)$ , a value close to  $\nu = 0.592$  for  $\epsilon = 1$ . More precise techniques give  $\nu = 0.588$ ,<sup>38</sup> a value very close to the Flory estimation.

The analogy with critical phenomena has been exploited by Hanke, Eisenriegler, and Dietrich to compute the contribution from a depleted polymer solution to the surface excess energy.<sup>39</sup> Results to first order in  $\epsilon$  give for the spontaneous curvature

$$\Delta c_0 = 0.125 \frac{k_B T}{\kappa} \rho_b R^2 (1 - 0.131\epsilon) + \mathcal{O}(\epsilon^2) \quad (20)$$

and for the elastic constants

$$\Delta\kappa = -0.133k_B T \rho_b R^3 (1 - 0.0713\epsilon) + \mathcal{O}(\epsilon^2) \quad (21)$$

$$\Delta\bar{\kappa} = 0.266k_B T \rho_b R^3 (1 - 0.177\epsilon) + \mathcal{O}(\epsilon^2) \quad (22)$$

with  $\rho_b$  the bulk concentration and  $R^2 = N^{2\nu} a^2/3$ . The case of Gaussian chains corresponds to  $\epsilon = 0$ . From the scaling point of view one gets results similar to hard sphere depletion. The depletion of soft and hard spheres are of the same order of magnitude, albeit with different numerical prefactors.

## 4. ADSORPTION OF POLYMERS

The contribution of adsorbed polymers to the elastic constants of fluid bilayers was first discussed at the scaling level by de Gennes,<sup>40</sup> who did not however calculate the amplitude or the sign of the contributions. A more systematic approach was developed by Brooks et al.<sup>41</sup> who studied the renormalization of the elastic constants both at the mean-field and the scaling levels.

Reversible adsorption of polymer chains can be described by an energy density which is a functional of the local monomer volume fraction  $\phi$  through the order parameter  $\psi = \phi^{1/2}$ . Hereafter  $a$  is the size of a monomer,  $\rho$  the monomer number density, and  $\phi = \rho a^3$ . At fixed chemical potential the Cahn-de Gennes free energy can be

written as<sup>42</sup>

$$F[\psi] = -k_B T \frac{\gamma}{a^2} \int dS \psi^2 + \frac{k_B T}{a^3} \int dV \left( \frac{a^2}{6} (\nabla \psi)^2 + \frac{1}{2} \tilde{v} (\psi^2 - \psi_b^2)^2 \right) \quad (23)$$

The first integral describes the direct interaction with the surface, the dimensionless parameter  $\gamma$  represents the contact energy between the monomers and the wall. According to the sign of  $\gamma$ , this energy functional can describe adsorption or depletion. The gradient term is related to the chain connectivity and the last term in the functional describes volume excluded interactions.  $\tilde{v} = v/a^3$  is the excluded volume parameter, in fact the second virial coefficient related to the Flory interaction parameter  $\chi$  through  $v = (1 - 2\chi)a^3$ .  $\psi_b$  is the bulk value of the order parameter.

Polymer adsorption is different from other adsorption problems due to chain connectivity. Indeed adsorption of only a few monomers of a given chain restrain close to the surface all the monomers belonging to that chain. The interfacial energy depends thus on the adsorbed concentration profile that extends far from the surface. Functional minimization of the energy density (23) provides an Euler-Lagrange differential equation for the profile

$$\frac{a^2}{6} \nabla^2 \psi - \tilde{v} \psi^3 + \tilde{v} \psi_b^2 \psi = 0 \quad (24)$$

with boundary conditions

$$\left. \frac{1}{\psi} \frac{\partial \psi}{\partial n} \right|_{\text{surf}} = -\frac{1}{2D} \quad (25)$$

where  $n$  is the normal to the surface. This condition defines the extrapolation length  $D = a/(12\gamma)$  that characterizes the strength of adsorption ( $\gamma > 0$ ) or depletion ( $\gamma < 0$ ). The extrapolation length is in principle also a function of the surface curvature, but this dependence can be neglected in the limit of infinitely narrow wall potentials. A second characteristic length of the problem is the correlation length  $\xi_b = a/(3v\rho_b)^{1/2}$  introduced by Edwards.<sup>36</sup> For concentrated or semidilute solutions,  $\xi_b$  determines the longest decay of the profile that reaches the bulk value for  $z \ll \xi_b$ . The screening length can also be described as a thermal “blob” size: For distances larger than  $\xi_b$  the excluded volume interactions are screened and the polymer chain correlations exhibit a gaussian behavior. In dilute solutions,  $\xi_b$  is simply given by the chain radius.

Brooks et al. solved the Euler-Lagrange Eq. (24) in the limit of weak adsorption  $\xi_b \ll D$  for cylindrical and spherical boundary conditions. The expansion of the excess surface energy leads to the spontaneous curvature value

$$\Delta c_0 = \frac{3}{8} \gamma^2 \frac{k_B T}{\kappa} \rho_b \xi_b^2 \quad (26)$$

To first order in the curvature the energy is lowered if the surface bends *towards* the solution, both for the adsorption and the depletion cases. Concerning elastic moduli renormalization, these authors found that polymer adsorption or depletion reduce the bending rigidity and increase the gaussian curvature constant

$$\Delta \kappa = -\frac{9}{8} \gamma^2 k_B T \rho_b \xi_b^3 \quad (27)$$

$$\Delta \bar{\kappa} = \frac{3}{4} \gamma^2 k_B T \rho_b \xi_b^3 \quad (28)$$

Equilibrium adsorption or depletion softens the membranes and increase the tendency of the membrane solution to the formation of bicontinuous structures with a high density of saddle point geometries. These authors discuss also the adsorption profiles beyond the mean-field level by using a modification of the energy functional suggested by de Gennes. The numerical resolution of the corresponding non-linear differential equations lead to qualitatively similar results, albeit with different exponents and prefactors. They also solve numerically the mean field, strong adsorption limit  $\xi_b \gg D$ , for which Clément et Joanny<sup>43</sup> provided later an analytical solution. For mean-field strong adsorption these authors obtained the following expressions

$$\Delta \kappa = -\frac{8}{9} k_B T \rho_b a \xi_b^2 \quad (29)$$

$$\Delta \bar{\kappa} = \frac{4}{3} k_B T \rho_b a \xi_b^2 \quad (30)$$

For both strong and weak adsorption the corrections to the elastic constants assume the form  $\sim k_B T \rho_b$  [length]<sup>3</sup>, the effective length depending on the adsorption regime. For weak adsorption where excluded volume effects are predominant, the corrections are proportional to  $\xi_b^3$ . Conversely, for strong adsorption the system is essentially two dimensional and the corrections become independent of  $\gamma$ : The correction factor is proportional to  $a \xi_b^2$ . It is worth stressing again that the corrections are independent of the interactions sign, they hold both for adsorption or depletion, provided that the equilibrium with the solution holds. At the opposite limit of irreversible adsorption the corrections have a logarithmic form  $\ln(\xi_b/D)$ .<sup>41</sup> More recently, chain finite size effects have also been considered.<sup>44</sup>

## 5. POLYMER-DECORATED MEMBRANES

In this section, we review the elastic properties of membranes decorated with polymer chains. Depending on the grafting density  $\sigma$ , one can define two different regimes that we now discuss.

### 5.1. High Grafting Density: The Brush Regime

When the average distance between the anchors is smaller than the radius of gyration of the polymers, the chains

adopt a stretched configuration. In their seminal works, Alexander and de Gennes use scaling arguments to describe properties of polymer brushes. For instance, the equilibrium height  $h$  of the layer is obtained by balancing the stretching energy of the chains with the excluded volume repulsion between monomers. In a mean-field description, the thickness of the brush scales as  $h \sim N\sigma^{1/3}$ , and the corresponding free energy per unit area is  $f \sim N\sigma^{5/3}$  (Ref. [45]). This approach neglects however intra-chain correlations, that were accounted for by de Gennes: In his picture, the chains are described as strings of blobs whose radius  $\xi$  is set by the grafting density,  $\xi \sim \sigma^{-1/2}$ . Each blob containing  $g \sim \xi^{5/3}$  monomers, the brush thickness is found to follow the same scaling law  $h \sim (N/g)\xi \sim N\sigma^{1/3}$ , but with a corresponding energy  $f \sim (N/g)k_B T\sigma \sim k_B TN\sigma^{11/6}$  (Ref. [46]).

These scaling ideas can be adapted to a polymer brush grafted to a membrane. The bending modulus scale as an energy and the excess bending modulus is  $\Delta\kappa \sim fh^2$ , with  $f$  the polymer brush free energy per unit area.<sup>47</sup> In a mean-field approach, the excess bending rigidity is then expected to scale as  $\Delta\kappa \sim \Delta\bar{\kappa} \sim N^3\sigma^{7/3}$ . Milner and Witten have evaluated more accurately the surface energy for spherical and cylindrical geometries,<sup>48</sup> they obtain

$$\Delta\kappa = k_B T \frac{9}{64} \left(\frac{12}{\pi}\right)^{1/3} N^3 (\sigma a^2)^{7/3} \quad (31)$$

$$\Delta\bar{\kappa} = -k_B T \frac{3}{35} \left(\frac{12}{\pi}\right)^{1/3} N^3 (\sigma a^2)^{7/3} \quad (32)$$

Using the blob picture, one finds a slightly different exponent,  $\Delta\kappa \sim \Delta\bar{\kappa} \sim N^3\sigma^{5/2}$ . Indeed, a careful evaluation gives<sup>49</sup>

$$\Delta\kappa = k_B T \frac{65}{72} N^3 (\sigma a^2)^{5/2} \quad (33)$$

$$\Delta\bar{\kappa} = -k_B T \frac{5}{18} N^3 (\sigma a^2)^{5/2} \quad (34)$$

However, recent numerical simulations<sup>47</sup> seem to indicate that both approaches under-estimate  $\Delta\kappa$ . Because of the high monomer volume fraction in the vicinity of the surface, the measured excess bending modulus actually scales with the grafting density as  $\sigma^{4/3}$ , but in all cases, the corrections are of the order of  $k_B T$  for a “dilute” brush close to the overlap density.

## 5.2. Low Grafting Density: The Mushroom Regime

At low grafting density, the excess free energy per unit area is simply proportional to the density,  $\Delta\gamma \sim k_B T\sigma$ . One then expects curvature corrections of the form  $\Delta\gamma = k_B T\sigma(1 + c_1 R_p/R + c_2 R_p^2/R^2)$ , with  $c_1, c_2$  some numerical constants. Here,  $R_p = N^\nu a$  is the typical size of the polymer chain, with  $\nu = 1/2$  for ideal chains and  $\nu = 3/5$  for chains in good solvent condition. The polymer contribution should therefore be larger in good solvent since the chains

are swollen by excluded-volume interactions. Dimensional analysis then predicts that the corrections should scale as  $\Delta\kappa \sim \Delta\bar{\kappa} \sim k_B T\sigma R_p^2$ , independently of the solvent quality. However, the details of chain architecture and solvent quality are relevant for the value and the sign of the prefactors, that we now discuss.

### 5.2.1. Polymers in Good and Theta Solvent

We first consider polymer chains anchored by one extremity to the membrane. Once the internal conformations of the polymer have been integrated out, the excess free energy per unit area of the decorated membrane is, for a single chain,

$$\Delta\gamma^{(i)} = -\frac{k_B T}{\mathcal{S}} \ln \left( \frac{\mathcal{Z}_N^{(i)}}{\mathcal{Z}_N^{(p)}} \right) \quad (35)$$

with  $\mathcal{Z}_N^{(i)}$  the partition function of a chain attached to a sphere ( $i = s$ ) or to a cylinder ( $i = c$ ). When the grafting density  $\sigma$  is low, inter-chains interactions can be neglected and different contributions simply sum up. The resulting spontaneous curvature is always negative

$$\Delta c_0 = -a_0 \frac{k_B T}{\kappa} \sigma R_p \quad (36)$$

where  $a_0$  depends on the solvent quality. Explicit calculations for Gaussian chains lead to  $a_0 = \sqrt{\pi/96} \simeq 0.181$ ,<sup>50</sup> and numerical methods for chains in good solvent give  $a_0 \simeq 0.168$ .<sup>51</sup> In both case, the configurational entropy of the chains increases if the surface bends away from the polymers. Using the notations of Ref. [51], the corrections to the bending moduli scale as

$$\Delta\kappa = 2a_\kappa k_B T\sigma R_p^2 \quad (37)$$

$$\Delta\bar{\kappa} = -2a_{\bar{\kappa}} k_B T\sigma R_p^2 \quad (38)$$

with  $a_\kappa = (\pi + 2)/24 \simeq 0.214$  and  $a_{\bar{\kappa}} = 1/6 \simeq 0.166$  for ideal chains,<sup>49</sup> and  $a_\kappa \simeq 0.200$  and  $a_{\bar{\kappa}} \simeq 0.153$  for chains in good solvent.<sup>51</sup> The linear increase of the bending rigidity with  $\sigma R_p^2$  has first been tested for decorated vesicles using micropipette technics<sup>52</sup> and carefully studied for decorated microemulsions.<sup>53,54</sup> Note that close to the overlap concentration  $\sigma^* \sim R_p^{-2}$ , the corrections are of the order of the thermal energy  $\Delta\kappa \sim \Delta\bar{\kappa} \sim k_B T$ , so that one continuously crosses over from the dilute (mushroom) to the concentrated (brush) regime.

### 5.2.2. Effect of Chain Architecture

In this section, we limit the discussion to ideal chains and consider four different architectures schematically drawn in Figure 2. We use the name “hair” for a polymer chain grafted by a single extremity (I), “siamese” molecule for a chain grafted by the median monomer (II), “loop” molecule for the case where both extremities are anchored (III), and “gemini” molecule for a transmembrane chain (IV). The

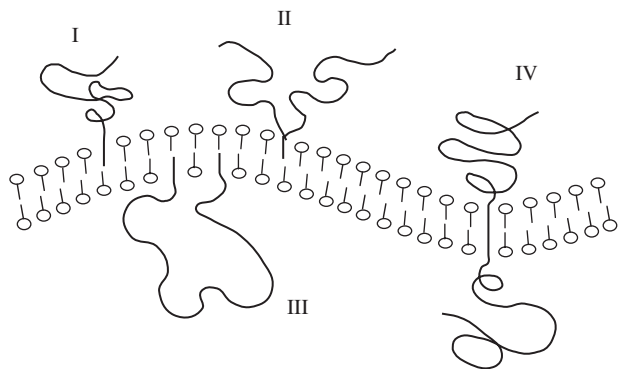


**Fig. 2.** Different architectures of the grafted chains: Hairs (I), siamese molecule (II), loop (III), and gemini (IV).

same contribution to the elastic moduli is obtained for hairs, siamese, and gemini molecules<sup>49,55</sup>

$$\Delta\kappa = \frac{\pi+2}{2} k_B T \sigma R_g^2 \quad (39)$$

$$\Delta\bar{\kappa} = -2k_B T \sigma R_g^2 \quad (40)$$

with  $R_g = Na^2/6$  the radius of gyration. Concerning the induced spontaneous curvature, it vanishes for gemini molecules because of symmetry reasons. As expected, the chain contribution to the spontaneous curvature is negative for the hairs<sup>50,55</sup>

$$\Delta c_0 = -\frac{\sqrt{\pi}}{4} \frac{k_B T}{\kappa} \sigma R_g \quad (41)$$

as well as for the siamese molecules<sup>50,55</sup>

$$\Delta c_0 = -\frac{\sqrt{2\pi}}{4} \frac{k_B T}{\kappa} \sigma R_g \quad (42)$$

The situation is slightly more subtle in the case of the loops. First, corrections with the opposite sign are found for the elastic moduli

$$\Delta\kappa = -k_B T \sigma R_g^2 \quad (43)$$

$$\Delta\bar{\kappa} = 2k_B T \sigma R_g^2 \quad (44)$$

An increase of  $\bar{\kappa}$  tend to stabilize saddle structures, that are indeed favorable for the loops (see Fig. 3), but the decrease of  $\kappa$  is not intuitive *a priori*. In particular, it is not clear whether this fact is characteristic of the loops or if it is an artefact of the Gaussian chain model. The second point is that there is no spontaneous curvature induced by loop polymers

$$\Delta c_0 = 0 \quad (45)$$

When the anchors are close to each other, the polymer forms an anchored ring and the membrane bends away from the chain. On the other hand, if both ends are far apart, the polymer is in a stretched state and then pulls on the membrane as shown in Figure 3. These two competing effects happen to compensate exactly if the anchors are free to probe all the possible configurations.<sup>32</sup>

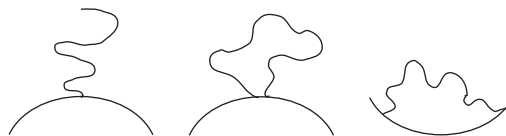


**Fig. 3.** A chain grafted by its extremity has more conformational entropy when the grafting surface is bent away from the chain. The same applies for loops when the grafting points are close to each other. However, when the grafting points are far away, the chain entropy is increased if the surface bends towards the chain.

To better understand this point, let us consider a loop attached on a sphere. The spontaneous curvature is in fact a function of the (horizontal) distance  $l$  between anchoring points<sup>55</sup>

$$\Delta c_0(l) = -\frac{\sqrt{\pi}}{8} \left(1 - \frac{2l^2}{R_{\parallel}^2}\right) \frac{k_B T}{\kappa} \frac{R_{\parallel}}{\mathcal{L}} \quad (46)$$

so that it vanishes at separation  $l_0 = R_{\parallel}/\sqrt{2}$ . Remarkably, in can be shown that the average of this quantity over all separations cancels out exactly

$$\begin{aligned} \langle \Delta c_0 \rangle &= \int_0^{\infty} dl \mathcal{P}(l) \Delta c_0(l) \\ &\propto \int_0^{\infty} dl \left(1 - \frac{2l^2}{R_{\parallel}^2}\right) e^{-l^2/2R_{\parallel}^2} = 0 \end{aligned} \quad (47)$$

a result illustrated in Figure 4.

### 5.2.3. Loops and Siamese Molecules: Effect of Anisotropy

As pointed out in the previous section, loop molecules present some intriguing features. The analysis can be refined and extended to the more general situation where the surface is locally described by its two principal radii of curvature  $R_1$  and  $R_2$ . We focus here more closely on the coupling between particle anisotropy and local surface conformation. This question has been studied quite

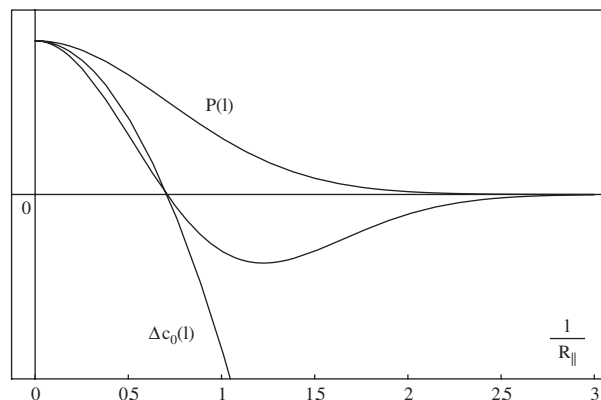


**Fig. 4.** The spontaneous curvature  $\Delta c_0$ , the probability  $\mathcal{P}(l)$  to find a conformation with a distance  $l$  between anchoring points and the product of both functions are represented in the figure. The integral of the product vanishes exactly.



generally in Ref. [56], and the results have been applied to both siamese molecules<sup>57</sup> and loop polymers.<sup>55</sup>

We first focus on loop molecules, and assume that the (projected) distance  $l$  between anchors is fixed. Experimentally, this configuration can be achieved by connecting the chains by a rigid (hydrophobic) spacer. The orientation of the molecule is then described by the vector  $\mathbf{l} = (x - x', y - y', 0)$ , and we call  $\theta$  the angle between  $\mathbf{l}$  and, for instance, the axis of principal curvature  $1/R_1$ . The discussion is restricted to the situation where both extremities are anchored symmetrically onto the surface,  $x' = -x$ ,  $y' = -y$ , and  $z = z' = -(R_1^{-2} \cos^2 \theta + R_2^{-2} \sin^2 \theta)l^2/4$ . The partition function of the chain can be evaluated following a perturbative method developed in Ref. [58]. Up to first order, the partition function is<sup>55</sup>

$$\begin{aligned} \mathcal{Z}_N(\mathbf{l}) = & \mathcal{Z}_N^{(0)} \exp(-l^2/R_{\parallel}^2) \\ & \times \left\{ 1 + \frac{\sqrt{\pi}R_{\parallel}}{4R_1} \left( 1 - \frac{4l^2 \cos^2 \theta}{R_{\parallel}} \right) \right. \\ & \left. + \frac{\sqrt{\pi}R_{\parallel}}{4R_2} \left( 1 - \frac{4l^2 \sin^2 \theta}{R_{\parallel}^2} \right) \right\} \quad (48) \end{aligned}$$

with  $R_{\parallel}^2 = 2Na^2/3$ , and  $\mathcal{Z}_N^{(0)}$  the partition function of the chain with both extremities grafted at the same point on a flat surface. The polymer contribution  $\mathcal{F} = -k_B T \ln \mathcal{Z}_N(\mathbf{l})$  to the free energy takes the following form

$$\mathcal{F} = \mathcal{F}_0 + \lambda \left( \frac{1}{R_1} + \frac{1}{R_2} \right) + \mu \left( \frac{1}{R_1} - \frac{1}{R_2} \right) \cos 2\theta \quad (49)$$

where the coefficients  $\lambda$  and  $\mu$  are given by

$$\lambda = -k_B T \frac{\sqrt{\pi}R_{\parallel}}{4} \left( 1 - \frac{2l^2}{R_{\parallel}^2} \right) \quad \text{and} \quad \mu = k_B T \frac{\sqrt{\pi}l^2}{2R_{\parallel}} \quad (50)$$

The anisotropy of the spontaneous curvature  $\mu/\lambda$  is vanishingly small for  $l$  of the order of the size of a monomer. However,  $\mu/\lambda$  is of order unity when  $l$  become comparable to the polymer size. Note that this ratio eventually diverges for  $l = R_{\parallel}/2$ .

Anisotropic inclusions promotes different spontaneous curvatures in the direction parallel or perpendicular to their orientation in the plane of the membrane. It has been shown that, whereas isotropic inclusions yield no spontaneous mean curvature when symmetrically adsorbed in a bilayer, anisotropic inclusions yield a spontaneous deviatoric bending  $R_1^{-1} - R_2^{-1} \neq 0$  by orienting at right angle across the bilayer. For  $\mathcal{N}$  inclusions anchored on each side of the membrane with density  $\sigma = \mathcal{N}/\mathcal{S}$ , the deviatoric contribution to the free energy (49) renormalizes the bending moduli according to<sup>56</sup>

$$\Delta\kappa = -\frac{1}{2}\Delta\bar{\kappa} = -\frac{\sigma\mu^2}{k_B T} \quad (51)$$

For siamese molecules, this contribution is<sup>57</sup>

$$\Delta\kappa = -\frac{9\pi}{16}k_B T \sigma R_g^2 \quad (52)$$

and it is found for the loops<sup>55</sup>

$$\Delta\kappa = -\frac{\pi}{4}k_B T \sigma \frac{l^4}{R_{\parallel}^2} \quad (53)$$

The effect of anisotropic gaussian inclusions is then to decrease the bending modulus  $\kappa$  and to increase the Gaussian modulus  $\bar{\kappa}$ . This can lead to interesting applications since the deviatoric contribution to the bending energy induces, above a concentration threshold, an ‘‘egg-carton’’ instability in flat membranes and a vesicle instability yielding long wormlike shapes.<sup>56</sup> Also interesting might be the possibility of changing the solvent quality, since excluded volume effects can change the sign of the siamese molecule contribution to the bending rigidity, as recently shown by Monte Carlo simulations.<sup>59</sup>

## 6. GRAFTED POLYMERS AS MINIATURIZED PRESSURE TOOLS

Achieving control of membrane shape and topology is of crucial importance to regulate function and performance of many systems in biology, physics, or chemical sciences. The design of a kit of versatile microscopic tools for tuning the shape of fluid membranes relies ultimately on the possibility of tailoring molecules for applying a given, well-chosen force, to the self-assembled surface. Here we discuss the ability of grafted polymers to perform as mesoscopic pressure patches. When a polymer chain is brought to the neighbourhood of a repulsive, impenetrable wall, the number of conformations available to the chain is reduced. Such a reduction of configurational entropy creates a non-homogeneous pressure field acting on the wall in a region comparable to the polymer size. In the case of a Gaussian end-grafted chain, the entropic pressure can be obtained by calculating the virtual work of an arbitrary deformation of the grafting surface. The pressure has the radially symmetric form<sup>60,61</sup>

$$p(r) = \frac{k_B T}{2\pi r^3} \left( 1 + \frac{r^2}{2R_g^2} \right) \exp \left\{ -\frac{r^2}{4R_g^2} \right\} \quad (54)$$

with  $r$  the in-plane distance from the grafting point. Close to the grafting point, the pressure can be as high as  $10^7$  Pa for  $a = 0.3$  nm at room temperature  $T = 300$  K. The pressure strength sharply decay from the center as  $p(r) \sim k_B T r^{-3}$ , and vanishes exponentially for distances larger than the polymer size. The  $r^{-3}$  dependance is the natural scaling for the pressure, and it can be shown that it still holds for chains with excluded volume.<sup>62</sup> The total force  $f$  exerted by the polymer onto the surface,  $f = \int_0^\infty 2\pi r p(r) dr \simeq k_B T/a$  is of the order of a few pN. The



grafted monomer exerts a point force  $-f$  that ensures mechanical equilibrium.

The forces describe above can be applied to a wide class of surface, provided that grafting of nonadsorbing chains is feasible. In membrane systems with vanishing surface tension, only the curvature rigidity will resist the polymer pressure. As a consequence, a fluid membrane will deform with a profile that is a compromise between applied pressure and elastic restoring forces. The resulting deformation close to the center of the pressure patch has a characteristic cone shape.<sup>60,61</sup> Far from the grafting point, the profile relaxes with a shape that depends essentially on the particular system under consideration (vesicle, supported membrane, ...).<sup>62</sup>

Different degrees of homogeneity for the pressure, and therefore different induced deformations, can be conceived by changing solvent quality,<sup>62</sup> chain architecture,<sup>63</sup> chain rigidity,<sup>64</sup> or electrostatic interactions. Even at neutral surfaces, a charged polymer is repelled by its image charge. The Maxwell pressure, which originate from the distortion of the electric field by the dielectric discontinuity, also act as a pressure patch. Combination of both entropic and electrostatic pressures should further enhance the possibility of designing customized mesoscopic force tools, suitable for many different applications.

## 7. CONCLUSIONS AND PERSPECTIVES

We presented in this paper a short review of the entropic interactions between soft objects of the nanoworld. Softness at this level translates into a high susceptibility to thermal forces, and many of the configurations and geometries adopted by such objects can be understood with theories developed at the crossroads of Physics, Chemistry, and Biology. Understanding brings also the possibility to actually predict and control such structures, a feature that will certainly appeal to future work in this field.

## References and Notes

- D. H. Everett, *Basic Principles of Colloid Science*, Royal Science of Chemistry Paperbacks, London (1988).
- J. N. Israelachvili, *Intermolecular and Surface Forces*, Academic Press, New York (1992).
- F. Evans and H. Wennerström, *The Colloidal Domain*, Wiley-VCH, New York (1998).
- D. D. Lasic, in *Structure and Dynamics of Membranes*, edited by R. Lipowsky and E. Sackmann, Elsevier, Amsterdam, The Netherlands (1995), Vol. 1A.
- B. Alberts, D. Bray, A. Johnson, J. Lewis, M. Raff, K. Roberts, and P. Walter, *Molecular Biology of the Cell*, Garland, New York (2002).
- W. Helfrich, *Z. Naturforsch.* 28c, 693 (1973).
- S. Safran, *Statistical Thermodynamics of Surfaces, Interfaces and Membranes*, Addison-Wesley, Reading, MA (1994).
- H. Lodish, A. Berk, S. L. Zipurski, P. Matsudaira, D. Baltimore, and J. Darnell, *Molecular Cell Biology*, Freeman, New York (2000).
- J. C. van de Pas, Th. M. Olsthoorn, F. J. Schepers, C. H. E. de Vries, and C. J. Buytenhek, *Coll. Surf. A* 85, 221 (1994).
- H. E. Warriner, S. H. J. Idziak, N. L. Slack, P. Davidson, and C. R. Safinya, *Science* 271, 969 (1996).
- Y. Yang, R. Prudhomme, K. M. McGrath, P. Richetti, and C. M. Marques, *Phys. Rev. Lett.* 80, 2729 (1998).
- G. Bouglet, C. Liguore, A.-M. Belloccq, E. Dufourc, and G. Mosser, *Phys. Rev. E* 57, 834 (1998).
- R. Joannic, L. Auvray, and D. D. Lasic, *Phys. Rev. Lett.* 78, 3402 (1997).
- H. Ringsdorf, J. Venzmer, and F. Winnik, *Angew. Chem. Int. Ed. Engl.* 30, 315 (1991).
- M. E. Cates, *Nature* 351, 102 (1991).
- V. Frette, I. Tsafrir, M.-A. Guedeau-Boudeville, L. Jullien, D. Kandel, and J. Stavans, *Phys. Rev. Lett.* 83, 2465 (1999).
- F. Martin and D. D. Lasic (eds.), *Stealth Liposomes*, CRC Press, New York (1995).
- U. Seifert, *Adv. Phys.* 46, 13 (1997).
- P. B. Canham, *J. Theor. Biol.* 26, 61 (1970); W. Helfrich, *Z. Naturforsch.* 28c, 693 (1973).
- S. T. Milner, T. A. Witten, and M. E. Cates, *Macromolecules* 22, 853 (1989).
- R. Podgornik, *Europhys. Lett.* 21, 245 (1993).
- A. Hanke, E. Eisenriegler, and S. Dietrich, *Phys. Rev. E* 59, 6853 (1999).
- M. Breidenich, R. R. Netz, and R. Lipowsky, *Europhys. Lett.* 49, 431 (2000).
- M. Doi and S. F. Edwards, *The Theory of Polymer Dynamics*, Clarendon Press, Oxford (1986).
- P.-G. de Gennes, *Scaling Concepts in Polymers Physics*, Cornell University Press, Ithaca, NY (1979).
- W. B. Russel, D. A. Saville, and W. Schowalter, *Colloidal Dispersions*, Cambridge University Press, Cambridge, NY (1989).
- F. C. Badwen, N. W. Pirie, J. D. Bernal, and I. Fankuchen, *Nature* 138, 1051 (1936).
- L. Onsager, *Ann. N.Y. Acad. Sci.* 51, 627 (1949).
- L. Auvray, *J. Phys. (France)* 42, 79 (1981).
- K. Yaman, P. Pincus, and C. M. Marques, *Phys. Rev. Lett.* 78, 4514 (1997).
- K. Yaman, M. Jeng, P. Pincus, C. Jeppesen, and C. M. Marques, *Phys. A* 247, 159 (1997).
- R. Lipowsky, H.-G. Döbereiner, C. Hiergeist, and V. Indrani, *Physica A* 249, 536 (1998).
- R. Lipowsky and H.-G. Döbereiner, *Europhys. Lett.* 43, 219 (1998).
- W. Kuhn, *Kolloid. Z.* 68, 2 (1934).
- P. Flory, *J. Chem. Phys.* 17, 303 (1949).
- S. F. Edwards, *Proc. Phys. Soc.* 85, 613 (1965).
- P.-G. de Gennes, *Phys. Lett. A* 38, 339 (1972).
- J. C. le Guillou and J. Zinn-Justin, *Phys. Rev. D* 15, 1544 (1977).
- A. Hanke, E. Eisenriegler, and S. Dietrich, *Phys. Rev. E* 59, 6853 (1999).
- P.-G. de Gennes, *J. Phys. Chem.* 94, 8407 (1990).
- J. T. Brooks, C. M. Marques, and M. E. Cates, *J. Phys. II (France)* 1, 673 (1991).
- P.-G. de Gennes, *Macromolecules* 14, 1637 (1981).
- F. Clément et J.-F. Joanny, *J. Phys. II (France)* 7, 973 (1997).
- K. I. Skau and E. M. Blokhuis, *Macromolecules* 36, 4637 (2003).
- S. Alexander, *J. Phys. (France)* 38, 983 (1977).
- P.-G. de Gennes, *J. Phys. (France)* 37, 1443 (1976).
- M. Laradji, *Europhys. Lett.* 60, 594 (2002).
- S. T. Milner and T. A. Witten, *J. Phys. (France)* 49, 1951 (1988).
- C. Hiergeist and R. Lipowsky, *J. Phys. II (France)* 6, 1465 (1996).
- R. Lipowsky, *Europhys. Lett.* 30, 197 (1995).
- T. Auth and G. Gompper, *Phys. Rev. E* 68, 051801 (2003).
- E. Evans and W. Rawicz, *Phys. Rev. Lett.* 79, 2379 (1997).
- H. Endo, J. Allgaier, G. Gompper, B. Jakobs, M. Monkenbusch, D. Richter, T. Sottmann, and R. Strey, *Phys. Rev. Lett.* 85, 102 (2000).

54. J. Appell, C. Ligoure, and G. Porte, *J. Stat. Mech.: Theor. Exp.* P08002 (2004).
55. T. Bickel, Ph.D. Thesis, Université Strasbourg (2001), p. 1. This document (in French) can be downloaded from the website: <http://tel.ccsd.cnrs.fr/>.
56. J.-B. Fournier, *Phys. Rev. Lett.* 76, 4436 (1996).
57. C. M. Marques and J.-B. Fournier, *Europhys. Lett.* 35, 361 (1996).
58. R. Podgornik, *Europhys. Lett.* 21, 245 (1993).
59. T. Auth and G. Gompper, *Phys. Rev. E* 72, 031904 (2005).
60. T. Bickel, C. M. Marques, and C. Jeppesen, *Phys. Rev. E* 62, 1124 (2000).
61. M. Breidenich, R. R. Netz, and R. Lipowsky, *Europhys. Lett.* 49, 431 (2000).
62. T. Bickel, C. Jeppesen, and C. M. Marques, *Eur. Phys. J. E* 4, 33 (2001).
63. A. Nicolas, B. Portelli, A. Halperin, and B. Fourcade, *Europhys. Lett.* 53, 687 (2001).
64. K. Guo, F. Qiu, H. Zhang, and Y. Yang, *J. Chem. Phys.* 123, 074906 (2005).

Received: 15 October 2005. Revised/Accepted: 7 December 2005.